Assignment III Lens Antenna

EE4725 Quasi Optical Systems

Petar V. Peshev, p.v.peshev@student.tudelft.nl
Department of Electrical Engineering, Mathematics, and Computer Science,
Delft University of Technology, Delft, The Netherlands

Abstract

In this assignment, a lens antenna, made of silicon with $\epsilon_r = 11.9$, has a planar feed with $n = 4$. The antenna has a diameter $D = 6\lambda_0$. Furthermore, the frequency of operation is $f = 50\ GHz$.

I. Simulations

The scripts used to simulate the lens antenna are in the GIT repository Assignment III Repository; and the library developed and used in the scripts is in quasi-optics-library. To run the simulations either place the script and library repositories in the same parent folder or change the library path in the simulation scripts.

II. Feed Far-Field Pattern of Planar Antenna

The lens antenna has a planar feed, which has an electric far-field given by

$$E_{feed}^{FF}(\theta, \phi) = \cos^n \theta (\cos \phi \hat{\theta} - \sin \phi \hat{\phi}) \frac{e^{-jk_d r}}{2\pi r}, \tag{1}$$

where the far-field is evaluated in the dielectric of the lens and $n = 4$; consequently the propagation constant k_d is calculated for the wave in the lens's dielectric.

The UV plot of the feed's electric far-field in the lens's silicon medium (permittivity $\epsilon_r = 11.9$) at the operating frequency $f = 180$ GHz is visualized in Fig.1; furthermore, its E-plane is plotted in Fig.2 as a function of θ. The planar feed's radiation pattern has one lobe over the valid spherical domain ($\theta = [0\ \ 90°]$ and $\phi = [0\ \ 360°]$) with maximum at $\theta = 0°$ and $\phi = 0°$. Moreover, the 3dB beamwidth of the feed is around $50°$. This feed is useful because it radiates an overall uniform field with no side-lobes over the considered elevation angle domain; the beamwidth can be optimized by changing n.

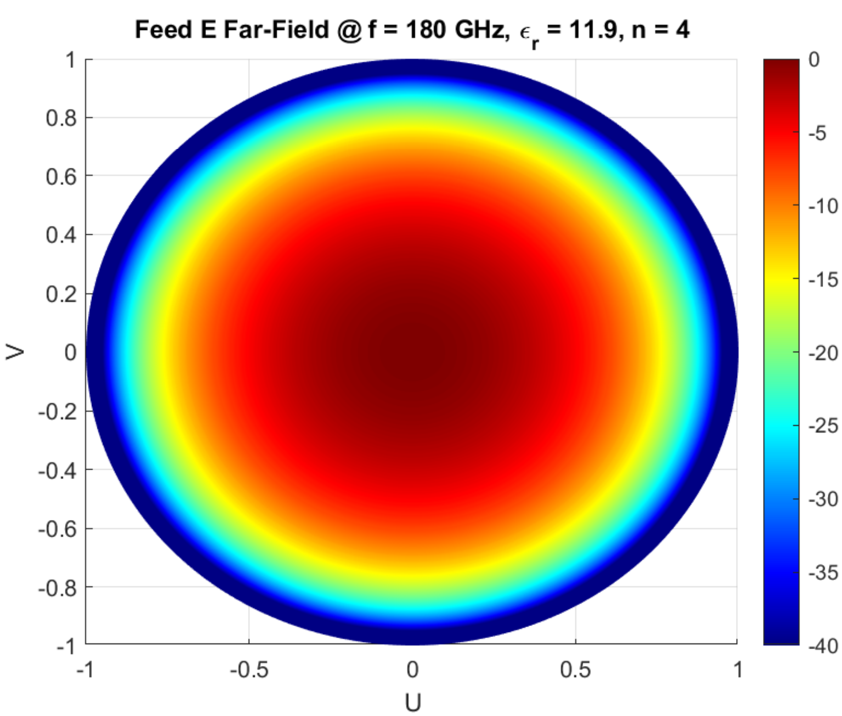

Fig. 1. Feed's electric far-field $\vec{E}_{feed}^{FF}$ at silicon medium with $\epsilon_r = 11.9$ in decibels dB and normalized to the maximum value, for a frequency $f = 180$ GHz and $n = 4$; visualized in UV coordinates.

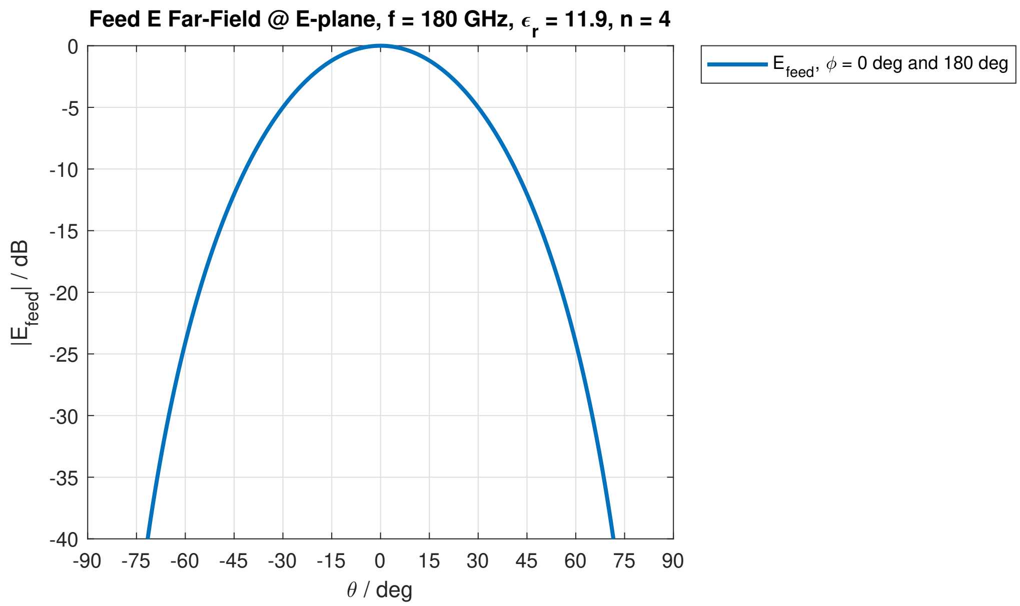

Fig. 2. Feed's electric far-field $\vec{E}^{FF}_{feed}$, for $\phi = 0°$ and $180°$, at silicon medium with $\epsilon_r = 11.9$ in decibels dB and normalized to the maximum value, for a frequency $f = 180$ GHz and $n = 4$; visualized in UV coordinates.

III. Fresnel Transmission Coefficient For Flat Interface

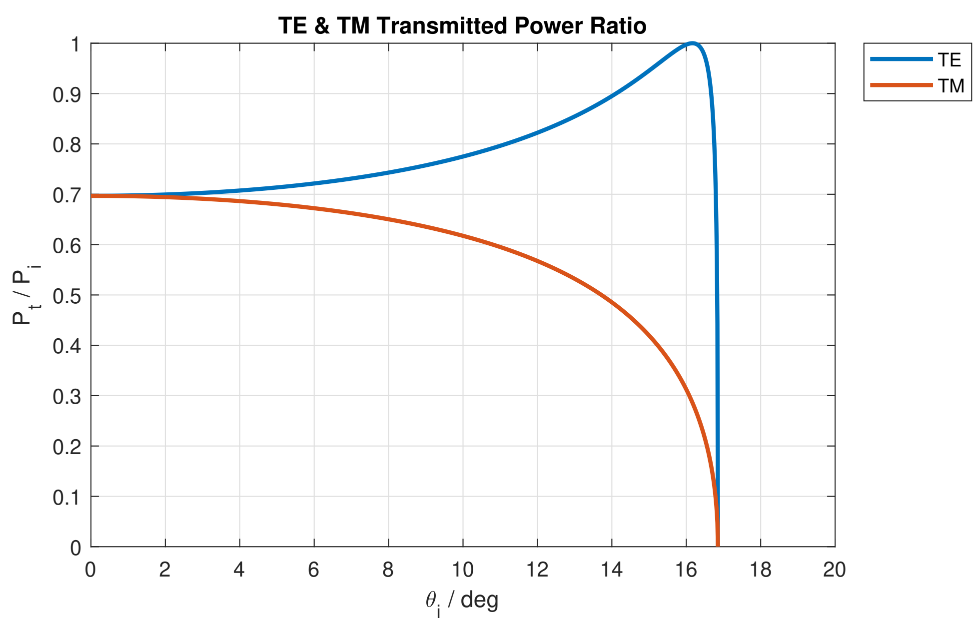

Fig. 3. Transmitted power ratio as a function of the incident angle θ_i for the transverse electric (TE) and transverse magnetic (TM) components. The critical angle for the flat interface is at $\theta_i = 16.85°$.

The TE and TM reflection coefficients are respectively

$$\tau^{TE} = \frac{2\zeta_0 \cos\theta_i}{\zeta_0 \cos\theta_i + \zeta_d \cos\theta_t}, \tag{2a}$$

$$\tau^{TM} = \frac{2\zeta_0 \cos\theta_i}{\zeta_0 \cos\theta_t + \zeta_d \cos\theta_t}, \tag{2b}$$

where ζ_0 and ζ_d are the wave impedance in free space (assuming the lens antenna is placed in free space) and the lens's dielectric respectively, and θ_i and θ_d are the incident and transmission angle respectively. The transmitted power ratio for TE and TM respectively are

$$\frac{P_t^{TE}}{P_i^{TE}} = |\tau^{TE}|^2 \frac{\zeta_d \cos\theta_t}{\zeta_0 \cos\theta_t}, \tag{3a}$$

$$\frac{P_t^{TM}}{P_i^{TM}} = |\tau^{TM}|^2 \frac{\zeta_d \cos\theta_t}{\zeta_0 \cos\theta_i}. \tag{3b}$$

The transmitted power ratio for the TM and TE polarization from silicon medium to free space are plotted in Fig.3 as a function of the incident angle θ_i. As a consequence of the wave being incident on an interface from a medium with higher permittivity towards a medium with lower permittivity, above a certain critical angle, known as the critical angle, the wave experiences total internal reflection. This critical angle for silicon is around $\theta_c = 16.85°$, observed on the plot. When the permittivity of the first medium increases, the critical angle decreases. Moreover, the TE polarization transmission ratio grows and experiences total transmission shortly before the critical angle. The angle at which the TE polarization experience total transmission is known as the Brewster's angle. The TM polarization does not experience total transmission. Finally, the critical angle and Brewster's angle are respectively

$$\theta_c = \sin^{-1}\frac{1}{\sqrt{\epsilon_r}}, \tag{4a}$$

$$\theta_B = \tan^{-1}\frac{1}{\sqrt{\epsilon_r}}. \tag{4b}$$

IV. Fresnel Transmission Coefficient For Lens Interface

For a untruncated elliptical lens, the maximum lens elevation angle at which transmission occurs is

$$\theta_0 = 90° - \theta_c, \tag{5}$$

where the critical angle is as defined in Eq.4a.

The transmitted power ratio for the TM and TE polarization from an elliptical silicon lens with diameter $D = 6\lambda$ to free space is plotted in Fig.4 as a function of the lens's elevation angle θ. The maximum lens's angle at which transmission occurs is $\theta_0 = 73.15°$. Furthermore, the TE polarization again experiences total transmission. In fact, the pattern is similar to the one for flat interface, however, it is stretched out to larger lens elevation angle. Therefore, this shape is useful as it allows larger domain of transmission.

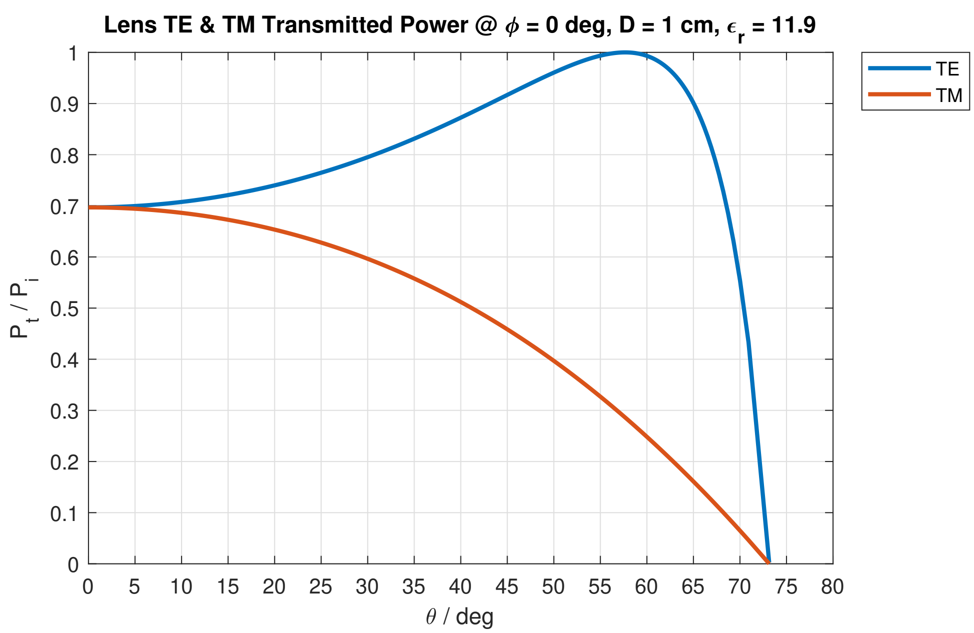

Fig. 4. Transmitted power ratio as a function of the incident angle θ_i for the transverse electric (TE) and transverse magnetic (TM) components. The critical angle for the lens interface is at $\theta_i = 73.15°$.

V. Equivalent Current Distribution

The equivalent aperture current distribution, using Schelkunoff's formulation and the image theorem, for an elliptical lens is

$$\vec{J}_s(\rho) \approx \hat{z} \times \vec{H}_t \mid_S = -\frac{2}{\zeta_0}(\tau^{TM}(\theta)E^{\theta}_{feed}(\vec{\rho})\hat{\rho} + \tau^{TE}(\theta)E^{\phi}_{feed}(\hat{\rho})\hat{\phi})\frac{S(\hat{\rho})}{r}, \tag{6}$$

where $S(\hat{\rho})$ is the spreading factor, the equivalent current is evaluated over the equivalent aperture surface, and the phase can be considered constant over surface and is neglected. The spreading factor is

$$S(\hat{\rho}) = \sqrt{\frac{\cos\theta_t(e\cos\theta - 1)}{\cos\theta_i(e - \cos\theta)}}, \tag{7}$$

where e is the eccentricity of the lens, and θ is the elevation angle inside the lens (calculated from the cylindrical coordinates used to define the lens); the spreading factor has to be equal to one over the whole domain. Moreover, the radial distance r is considered to be the one from the feed to the lens interface, while the radial distance of the wave propagating from the lens interface to the aperture surface r' is neglected. The $\hat{\theta}$ component of the feed's E-field is TM polarized and translates to the $\hat{\rho}$ component of the equivalent aperture current; on the other hand, the $\hat{\phi}$ component of the feed's E-field is TE polarized and translates to the $\hat{\phi}$ component of the equivalent aperture current. Effectively, there is a coordinate transformation from the spherical coordinate system defining the feed's field to a cylindrical coordinate system defining the equivalent aperture current. However, it must be noted that the cylindrical coordinates defining the aperture current are used to calculate the spherical coordinate system inside the lens. Furthermore, in case the phase term is not neglected, it can be calculated by $e^{-jk_0 r'}e^{-jk_d r}$, where the phase shift inside the lens's dielectric defined by $k_d r$ and the phase shift for the transmitted wave propagating towards the equivalent aperture surface defined by $k_0 r'$ are added. Finally, the equivalent aperture current is transformed to rectangular coordinates through coordinate vector transformation.

The x and y-components of the equivalent aperture electric current density for the elliptical lens antenna, made of silicon, truncated at $\theta_0 = 40°$, and having a diameter $D = 1$ cm, are plotted in Fig.5 in rectangular coordinates. The $y-component$ is more than 25 dB lower than the maximum magnitude of the x-component. Therefore, the equivalent current is mainly oriented in the x-direction. Moreover, the magnitude of the current in the x-component is larger at the middle of the lens and decreases by a larger factor with y. Consequently, the equivalent aperture current exhibits an elliptical shape.

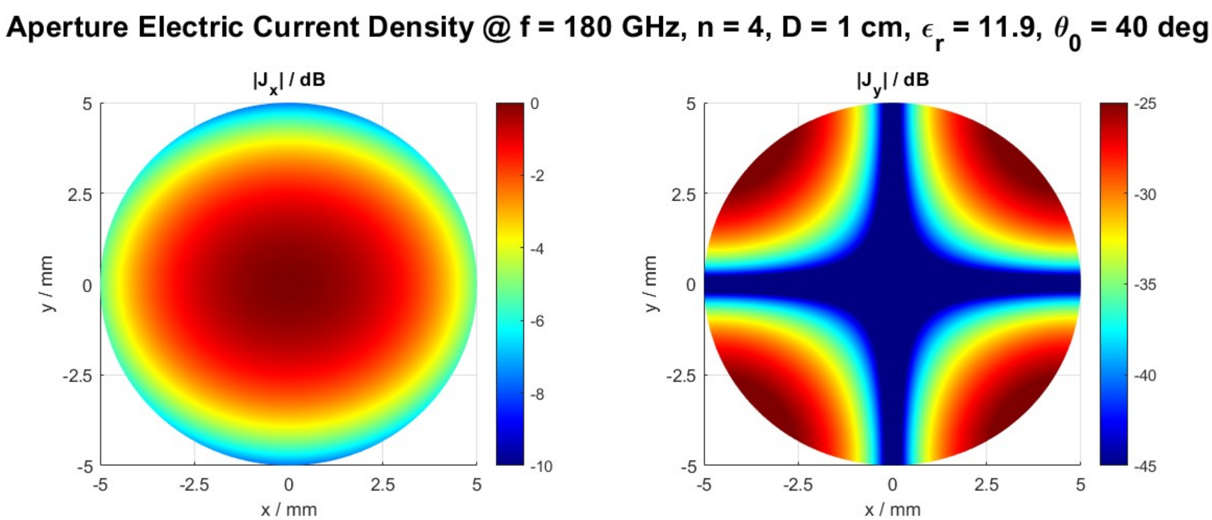

Fig. 5. Equivalent aperture current distribution's J_{eq} x and y-components plotted in Cartesian coordinates for silicon lens with $\epsilon_r = 11.9$, planar feed with $n = 4$, and truncated lens at $\theta_0 = 40°$. The x and y-components are normalized to the same magnitude.

VI. Far-Field Pattern of Lens

The electric far-field of the lens antenna is evaluated by the multiplication of the Spectral Green's function with the Fourier transform of the equivalent aperture current and is

$$\vec{E}^{FF}(\vec{r_f}) = jk_{z0}\bar{G}^{EJ}(k_{x0}, k_{y0})\tilde{\mathbf{J}}_S(k_{x0}, k_{y0})\frac{e^{-jk_0 r_f}}{2\pi r_f}, \tag{8}$$

where the field is evaluated in the far region of the lens at radial distance r_f, k_{x0}, k_{y0}, and k_{z0} are the x, y, and z components of the wave vector in free space respectively, $\bar{G}^{EJ}$ is the Spectral Green's function relating electric current density to electric field evaluated in free space, and $\tilde{\mathbf{J}}_S$ is the Fourier transform of the equivalent aperture current evaluated in free space. The Fourier transform $\tilde{\mathbf{J}}_S$ of the electric current density is

$$\mathbf{J}_S^{x/y}(k_{x0}, k_{y0}) = \int_0^{D/2}\int_0^{2\pi} J_S^{x/y}(\rho,\phi)e^{jk_{x0}\rho\cos\phi}e^{jk_{y0}\rho\sin\phi}\rho d\rho d\phi. \tag{9}$$

The electric far-field E^{FF} for the elliptical lens antenna, made of silicon, truncated at $\theta_0 = 40°$, and having a diameter $D = 1$ cm, is plotted in Fig.6. The radiation pattern is similar to an airy pattern, except artefacts appearing at $\theta_f = 90°$ (the valid domain of radiation is the upper half-space, therefore max elevation angle is $\theta_{f,max} = 90°$). The possible cause of these artefacts is the numerical far-field evaluation at $\theta_f = 90°$. Moreover, the lens E^{FF} is compared to the far-field of uniform current distribution (airy radiation pattern), at the $\phi_f = 0°$ and $180°$, and $\phi = 90°$ and $270°$ planes, in Fig.7 as a function of the elevation angle θ_f. Compared to the far-field of a uniform current distribution, the lens's far-field is similar, however it has slightly larger main-lobe beamwidth; yet, the side-lobes of the uniform pattern are higher than the side-lobes of the lens's far-field.

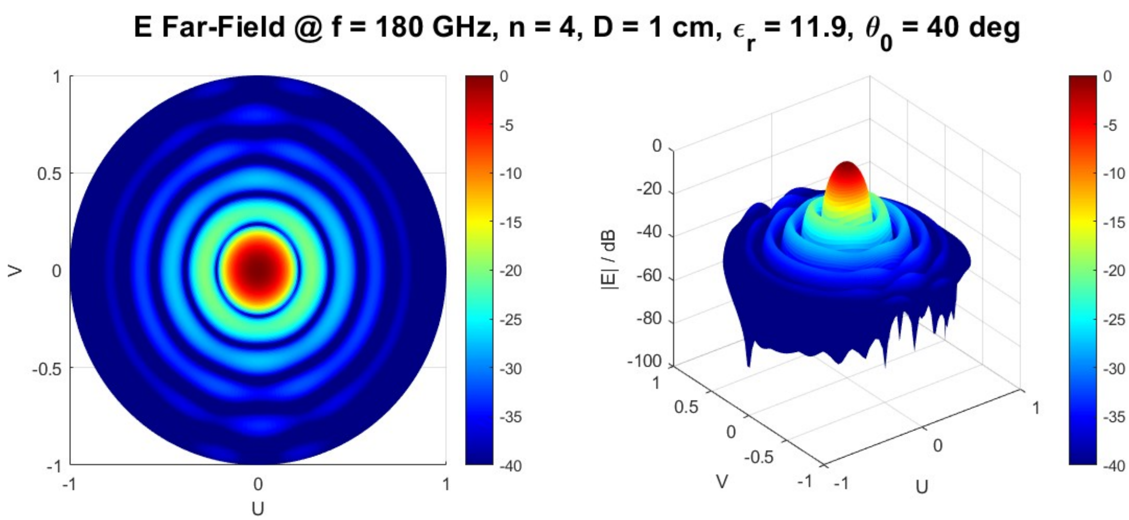

Fig. 6. Electric far-field E^{FF} of lens antenna made of silicon with $\epsilon_r = 11.9$, planar feed with $n = 4$, and truncated lens at $\theta_0 = 40°$; visualized in UV coordinates.

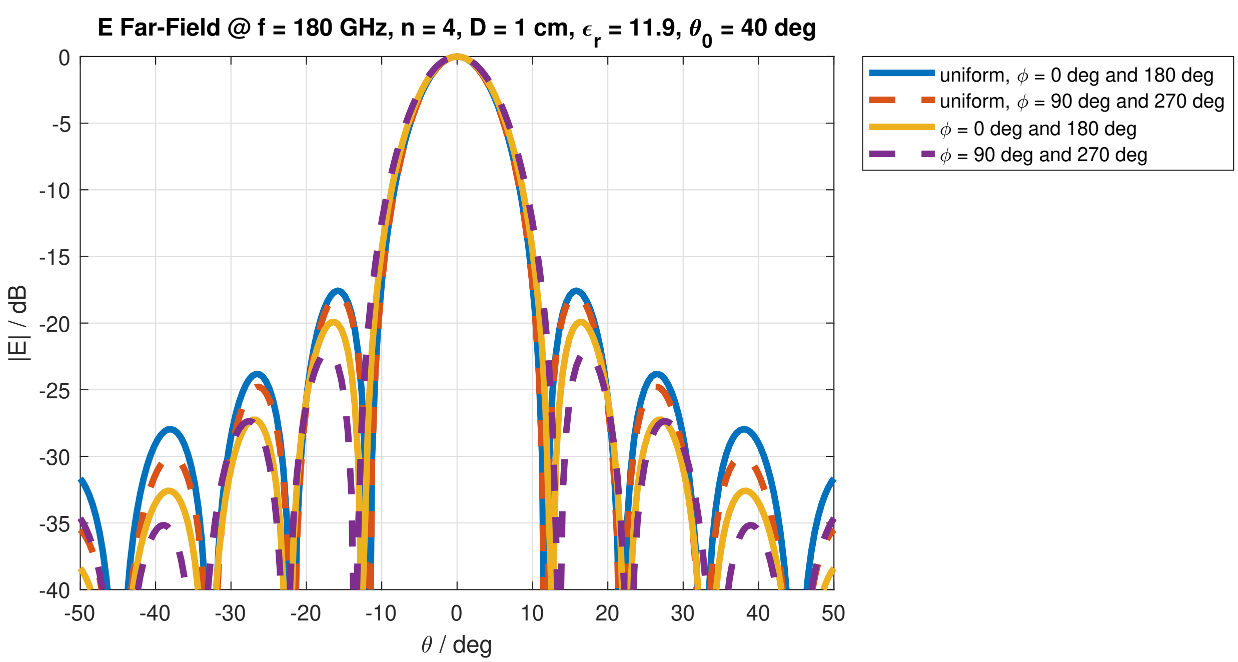

Fig. 7. Electric far-field E^{FF}, in main planes $\phi = 0°$ and $180°$ and $\phi = 90°$ and $270°$ as a function of the elevation angle θ, of lens antenna made of silicon with $\epsilon_r = 11.9$, planar feed with $n = 4$, and truncated lens at $\theta_0 = 40°$, compared to the pattern of uniform equivalent aperture current in the same planes.

VII. Directivity and Gain

The directivity is

$$\mathbb{D}(\theta_f, \phi_f) = 4\pi \frac{U(\theta_f, \phi_f)}{P_{rad}^{lens}}, \tag{10}$$

where $U(\theta_f, \phi_f)$ is the radiation intensity and P_{rad}^{lens} is the radiated power by the lens. Moreover, the radiation efficiency is

$$\eta_{rad} = \frac{P_{rad}^{lens}}{P_{rad}^{feed}}, \tag{11}$$

where P_{rad}^{feed} is the radiated power by the feed. Finally, using the directivity and radiation efficiency, the gain of the antenna is calculated

$$\mathbb{G}(\theta_f, \phi_f) = \mathbb{D}(\theta_f, \phi_f)\eta_{rad}. \tag{12}$$

For the elliptical lens antenna, made of silicon, truncated at $\theta_0 = 40°$, and having a diameter $D = 1$ cm, the efficiency, broadside directivity, and broadside gain are summarized in Table.I and are 63.46 %, 25.37 dB, and 23.39 dB respectively. Therefore, the antenna radiates 63.46 % of the feed's power.

TABLE I
EFFICIENCY, BROADSIDE DIRECTIVITY, AND BROADSIDE GAIN

η, D^{BS}, and G^{BS}	
	Figure
η	63.36 %
D	25.37 dB
G	23.39 dB